Ezio Venturino, Sergei Petrovskii. Spatiotemporal Behavior of a Prey-Predator System with a Group Defense for Prey. *Ecological Complexity*, 14, 37-47, 2013. DOI: 10.1016/j.ecocom.2013.01.004

Spatiotemporal Behavior of a Prey-Predator System with a Group Defense for Prey

Ezio Venturino[†] and Sergei Petrovskii[*]
[†]Dipartimento di Matematica "Giuseppe Peano",
Università di Torino, via Carlo Alberto 10, 10123 Torino, Italy
[*] Department of Mathematics, University of Leicester
Leicester, LE1 7RH, UK
E-mails: ezio.venturino@unito.it, sp237@leicester.ac.uk

Abstract

Group defense is a strategy widely employed by various species. We consider the effect of grouping on population persistence when animals join together in herds in order to provide a self-defense from predators. In literature, group defense is usually addressed in terms of individual behavioral responses. In this paper, we consider an alternative 'mean-field' approach which uses prey and predator densities as the dynamical variables. The model is essentially a predator-prey system but with an unconventional parametrization for the predation term. We discuss the outcomes of the ecosystem dynamics in terms of persistence and prey survival. In the spatially distributed model some specific spatio-temporal features are discovered.

Keywords: Patterns, predator-prey, group defense

1 Introduction

Social interactions in the animal kingdom have long been a focus of intensive research (Allee, 1938; Wilson, 1971; Fryxell and Lundberg, 1997). They may affect the community functioning in different ways, for instance, by creating a social hierarchy (Freeman et al., 1992; Sapolsky, 2005) or through emerging collective behaviour (Sendova-Franks et al., 2002), in particular through collective movement (Fernö et al., 1998). Especially the latter often result in animal grouping (Bode et al., 2011; Bertram, 1978) . However, grouping or aggregation may also appear for a variety of other reasons, (Grünbaum and Okubo, 1994), such as a more effective use of resources or aiming to provide an effective way to protect community members from an external threat (Bode et al., 2010), see also chapter 8 of Caro (2005) . In artificial life the problem of forming of flocks has been addressed mainly through the use of individual based models; for the latter see for instance Axelrod (1997); Macal and North (2009). In this paper, we consider the case when animals join together in herds in order to provide a self-defense from predators. In the review of Elgar (1989) the issue of the relationship between vigilance behavior and group size is addressed

and criticized. Our main goal is to reveal the combined effect of grouping and diffusing on the ecosystem's population dynamics in the spatio-temporal context. Of interest are issues such as pattern formation, ecosystem persistence and prey survival.

The group defense is usually addressed in terms of individual behavioral responses, when different members of the group have different and clearly defined tasks, and hence is thought to be best modeled using an individual-based modeling approach (Wood and Ackland, 2007; Bode et al., 2011). Other types of modeling, however, can be used which are closely related to individual based modeling, like statistical physics, cellular automata and stochastic processes, in which generic rules for the system dynamics can be explicitly stated (Malchow et al., 2008). An individual based approach is simulation-based, and therefore it often requires a lot of computational effort. Generic dependencies of the system's properties on parameter values are revealed only by extensive simulations, from which some generality of the results should be inferred.

In this paper, we consider an alternative approach when the effects of group defense on the population survival are considered in terms of a mean-field type model where the dynamical variables are the prey and predator densities. The model consists of two coupled diffusion-reaction equations where the predation term has an unconventional form. For the benefit of the reader, we first revisit the properties of the non-spatial system introduced in Ajraldi and Venturino (2009), Ajraldi et al. (2011). The bifurcation structure of the system as well as the bifurcation values of the controlling parameter is found analytically. We then extend the earlier results by revealing a 'mixed stability' of the extinction state. Basing on these results, we show that the system behavior is significantly different from that of traditional predator-prey models.

We then consider the spatially explicit system. We studied its properties by means of extensive computer simulations and found a variety of spatiotemporal patterns for different parameter ranges. We observed that the existence of the group defense may result in very long-living transients when the population size of the prey may show a steady growth over a long time before finally collapsing. Rather counter-intuitively, we also found that the spatial system may exhibit sustained oscillations in a parameter range where the corresponding nonspatial system goes extinct.

2 Background

2.1 Non-spatial model

Our investigation starts from a model recently proposed in Ajraldi and Venturino (2009) and analyzed further in Ajraldi et al. (2011) in which the hunting behavior of predators and the defensive strategy of prey are accounted for in a new way. Namely, it is assumed that while predators move freely in the environment actively searching for their prey, the latter instead gather together in herds for defensive purposes. Note that in Fryxell et al. (2007) a number of functional responses to model the same kind of situation are proposed: for the predation term they use nonlinearities expressed via rational functions; for the growth of the prey instead they use a Gompertz-like, or theta-logistic term. In reference to Ajraldi and Venturino (2009) and Ajraldi et al. (2011), the former choice represents a completely different approach, while the latter is somewhat related to the choice of the predation term. In fact, the main idea expounded in these latter works

is that the interaction between predators and prey affects mainly the prey individuals occupying the outermost positions in the herd. This assumption is novel and does not correspond to the usual assumption made in the original Lotka-Volterra model, nor in all the population models in which interactions are described. Since the prey individuals staying on the boundary of the herd are in number proportional to the length of the perimeter of the ground area occupied by the herd, and the perimeter is proportional to the square root of the area, if G denotes their density, it follows that generally the prey involved in hunting interactions with the predators are $\sqrt{G}$. In modeling terms, the consequence of the assumption is that the classical mass action term appearing in the Lotka-Volterra model is replaced by another unconventional nonlinear term containing a power law of the prey density. For generality sake, at first we formulate the model with a generic exponent $1 > \alpha > 0$, which we will specialize to the case $\alpha = \frac{1}{2}$ in the later numerical simulations. This allows to establish the sensitivity of a fundamental parameter to be defined later on with respect to the exponent of G. We obtain therefore the system

$$\frac{d}{d\tau}G(\tau) = r\left(1 - \frac{G(\tau)}{K}\right)G(\tau) - aG(\tau)^{\alpha}F(\tau)\ , \tag{1}$$

$$\frac{d}{d\tau}F(\tau) = -mF(\tau) + aeG(\tau)^{\alpha}F(\tau)\ . \tag{2}$$

The first equation describes the population dynamics of the prey; the first term on the right hand side expresses logistic growth with r being the per capita net reproduction rate and K the carrying capacity of the environment; the second term models the hunting process they are subject to by predators. The same term, scaled by the conversion coefficient e, appears also in the second equation, in which predators (described by their population density F) die out with mortality rate m in absence of their only food sources, namely the prey G. The exponent α thus represents a kind of aggregation efficiency.

The system (1–2) was considered in Ajraldi and Venturino (2009) and Ajraldi et al. (2011) for the special case $\alpha = \frac{1}{2}$. We summarize here the most important facts about (1–2) that apply to the more general case with an arbitrary $\alpha \in (0, 1)$. The equilibria are the system's extinction, the prey-only equilibrium and coexistence. The analysis of the system outcomes to distinguish between the various possible trajectories' behaviors can conveniently be done in terms of a certain parameter ρ where

$$\rho \equiv \frac{1}{K}\left(\frac{m}{ea}\right)^{\frac{1}{\alpha}} > 0. \tag{3}$$

For $\rho > 1$ the coexistence state is not feasible and the only biologically meaningful stable steady state is the prey-only equilibrium $(K, 0)$. The prey-only state and coexistence equilibria exhibit a transcritical bifurcation for $\rho = 1$. The coexistence state is feasible for $0 < \rho < 1$ and it is stable for $\rho_H < \rho < 1$ where

$$\rho_H = \frac{1-\alpha}{2-\alpha}. \tag{4}$$

At $\rho = \rho_H$ a Hopf bifurcation at the coexistence equilibrium arises, with this equilibrium becoming unstable and persistent oscillations arising around it when ρ attains smaller values. The equation (4) also shows the sensitivity of the Hopf bifurcation with respect

to the parameter α. The curve $\rho(\alpha)$ is in fact a concave branch of a hyperbola, smoothly dropping from the value $1/2$ at $\alpha = 0$ to zero for $\alpha = 1$. Therefore taking ρ as bifurcation parameter, qualitatively, the Hopf bifurcation point ρ_H on the curve $\rho(\alpha)$ moves toward the left for decreasing values of α.

It is therefore readily seen that the square root functional response used here has some resemblance with the saturating-type Holling type II or III responses, although it is not bounded above. The emergence of limit cycles appears thus to be related to the concavity of all these functions, rather than to the boundedness of the Holling type responses.

In addition, the stability features showing an exotic 'mixed stability' of the steady state at the origin are addressed by the following novel Theorem 1 and the subsequent Remarks 1 and 2.

Theorem 1. *Consider $0 < \alpha < 1$. Let $G_0 = G(0)$ and $F_0 = F(0)$ be the initial conditions for the system (1–2) and let S be the part of the system's phase plane defined as follows:*

$$S = \{(G, F) \mid G > 0,\ F > \tilde{F}(G)\} \quad where \quad \tilde{F}(G) = \frac{m + (1-\alpha)r}{a(1-\alpha)} G^{1-\alpha}\ . \tag{5}$$

Then for any $(G_0, F_0) \in S$ the prey goes extinct in finite time, i.e. the system's trajectory hits axis F at a certain $\hat{\tau} < \infty$.

Proof. We first consider Eq. (2) and note that, since G and F are non-negative,

$$\frac{d}{d\tau} F(\tau) = -mF(\tau) + aeG(\tau)^{\alpha} F(\tau) \geq -mF. \tag{6}$$

Therefore, by virtue of the comparison principle for ordinary differential equations, e.g. see Halil (2002), if $\hat{F}$ is the solution of the equation

$$\frac{d}{d\tau} \hat{F}(\tau) = -m\hat{F}(\tau),$$

corresponding to the same initial condition $\hat{F}(0) = F(0) = F_0$, then

$$F(\tau) \geq \hat{F}(\tau) = F_0 e^{-m\tau} \tag{7}$$

for any τ.

We now consider Eq. (1) and note that

$$\begin{aligned} \frac{d}{d\tau} G(\tau) &= r\left(1 - \frac{G(\tau)}{K}\right) G(\tau) - aG(\tau)^{\alpha} F(\tau) \leq rG - aG(\tau)^{\alpha} F(\tau) \\ &\leq rG - aG(\tau)^{\alpha} \hat{F}(\tau) = rG - G(\tau)^{\alpha} aF_0 e^{-m\tau}. \end{aligned} \tag{8}$$

Therefore, by virtue of the comparison principle (Halil, 2002), if $\hat{G}$ is the solution of the equation

$$\frac{d}{d\tau} \hat{G}(\tau) = r\hat{G} - \hat{G}(\tau)^{\alpha} aF_0 e^{-m\tau}, \tag{9}$$

corresponding to the same initial condition $\hat{G}(0) = G(0) = G_0$, then

$$G(\tau) \leq \hat{G}(\tau) \tag{10}$$

for any τ.

In order to solve Eq. (9), we introduce a new variable $W(\tau)$ as

$$\hat{G}(\tau) = W(\tau)e^{r\tau}. \tag{11}$$

Note that $W(0) = \hat{G}(0) = G_0$.

Having plugged (11) into (9), we obtain the following equation for W:

$$\frac{d}{d\tau}W(\tau) = -W(\tau)^{\alpha} a F_0 e^{-\beta\tau}, \tag{12}$$

where $\beta = m + (1-\alpha)r$.

Equation (12) is straightforward to solve resulting in

$$W(\tau)^{1-\alpha} = W(0)^{1-\alpha} - \frac{aF_0(1-\alpha)}{\beta}\left(1 - e^{-\beta\tau}\right). \tag{13}$$

Note that $W(0) > 0$ and the second term in the right-hand side of (13) is a monotonically increasing function of τ. It means that $W(\tau_*) = 0$ for a certain τ_* if and only if

$$W(0)^{1-\alpha} < \frac{aF_0(1-\alpha)}{\beta}\ . \tag{14}$$

Taking into account the relation (11) between W and $\hat{G}$, it is obvious that $W(\tau_*) = 0$ is equivalent to $\hat{G}(\tau_*) = 0$. Since $W(0) = G_0$, from (14) we obtain that $\hat{G}(\tau_*) = 0$ for any G_0 and F_0 satisfying the following condition:

$$F_0 > \frac{\beta}{a(1-\alpha)} G_0^{1-\alpha}\ , \tag{15}$$

where the explicit expression for the hitting time τ_* can be readily obtained from (13):

$$\tau_* = -\frac{1}{\beta}\log\left[1 - \frac{\beta}{aF_0(1-\alpha)} G_0^{1-\alpha}\right]. \tag{16}$$

Finally, we recall that $\hat{G}$ is an upper bound for $G(\tau)$; if $\hat{G}(\tau_*) = 0$ then $G(\tau_*) \le 0$, which actually means that $G(\tau)$ becomes zero for some $\hat{\tau} \le \tau_*$. Since $G(\tau)$ cannot become negative (because the axis $G = 0$ is a part of the G-isocline in the phase plane of system (1–2)), $G(\tau) \equiv 0$ for any $\tau \ge \hat{\tau}$. Inequality (15) therefore gives a sufficient condition for the prey species extinction. That completes the proof.

Remark 1. Once the prey goes extinct, the dynamics of the system (1–2) is reduced to the exponential decay of the predator, so that the system's trajectory in the phase plane asymptotically approaches the state $(0, 0)$ along the axis $G = 0$. Therefore, the meaning of the theorem is that, in the phase plane (G, F) of the system, there is a curvilinear sector close to the vertical axis, which appears to be the attraction basin for the origin; see Fig. 1. For the rest of the plane, the steady state $(0, 0)$ acts as a saddle point. The global structure of the phase plane is therefore very different from the one observed in the standard predator-prey systems.

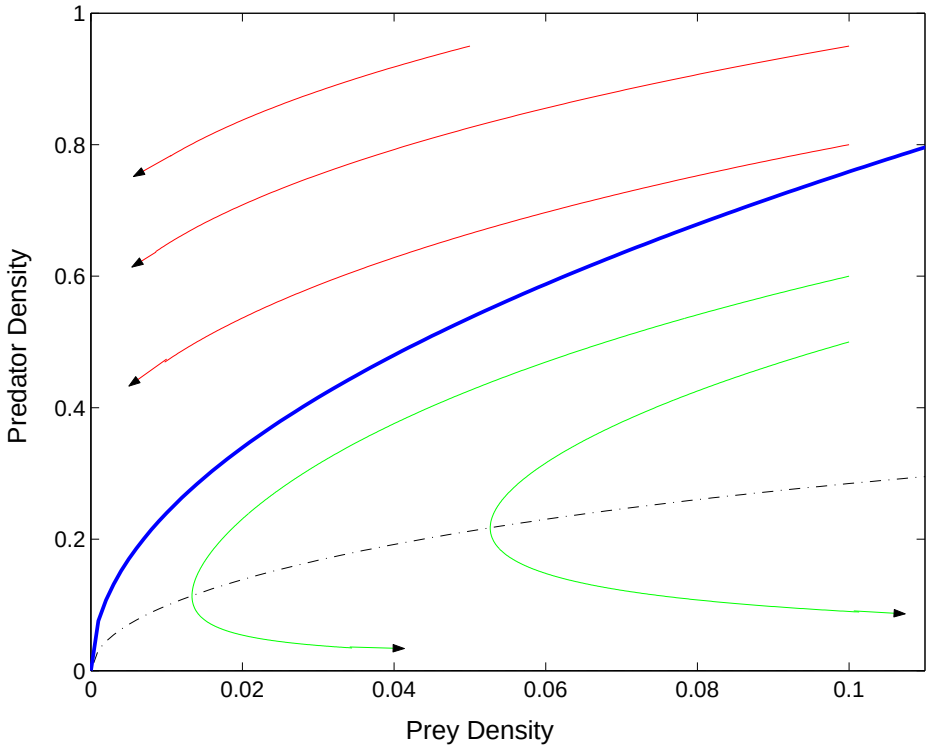

Figure 1: The phase plane of the system (1–2). The thick blue curve shows the boundary of the extinction domain S; see (5). For any initial conditions above this curve, the system trajectories (shown in red colour) hit the vertical axis, which means species extinction. For initial conditions below the curve, the trajectories (shown in green colour) approach an attractor in the interior of the phase plane (either the stable coexistence steady state or the stable limit cycle, depending on equation parameters) which means species persistence. The dashed-and-dotted curve shows the R-isocline of the system. The systems trajectories are obtained by solving Eqs. (1–2) numerically for parameters $K = r = a = 1$, $e = 0.8$, $m = 0.7$ and $\alpha = 0.5$.

Remark 2. Note that inequality (15) gives only a sufficient condition of prey extinction but not a necessary one. Therefore, the actual extinction domain in the (G, F) phase plane is somewhat larger than the domain S defined by (5); the extinction may happen as well for some $F_0 < \tilde{F}(G_0)$.

Thus this stability of "mixed type" of the origin always allows for extinction of the system in case the initial density F_0 of predator is sufficiently large, but for the species persistence in case F_0 is sufficiently small. We therefore infer that there must exist a separatrix separating the two different trajectories flows. Although we cannot obtain its explicit analytical expression, function $\tilde{F}(G)$ (see (5)) seems to provide a good approximation for it.

Remarkably, the chain of bifurcations does not end with the Hopf bifurcation. Numerical simulations show that a further decrease in ρ results in a nonlocal bifurcation: for a certain value $\rho_* < \rho_H$, the limit cycle collides with the separatrix and disappears. For any $\rho < \rho_*$ the system goes to extinction; the prey density decays to zero monotonically for the initial conditions chosen above the separatrix and it approaches zero in an oscillatory

manner if the initial values are taken below the separatrix.

2.2 Spatially explicit model

In a natural environment it is clear that prey gather together not just in one herd, but on a large territory we expect to find several groups of the same population wandering about. At the same time, predators are on the lookout for food and possibilities of hunting their prey. It is widely recognized that predators, when hunting collectively, do not accept newcomers as new individuals in their midst. However, such behavior is not matched by the large herbivores feeding in the savannas (FitzGibbon, 1989, 1990), nor in the aquatic environment (Magurran, 1990). It makes therefore sense to consider a spatial system in which rather than modeling each individual in the two populations, a reduction in scale is achieved by using the above model. We therefore consider two interacting populations in which the prey are allowed to gather together in herds. Each spatial location is meant as a large enough territory, in which exactly one bunch of prey can wander around as well as some individually behaving predators. Therefore, at each location in space, (1–2) constitutes the local, i.e. non-spatial, model for interactions. We need to describe the dynamics of the system in the larger environment. To this end, keeping in mind that the individualistic behavior of predators can easily be captured via a standard diffusion equation, as it has been the case for many such models (Malchow et al., 2008) the extension of (2) with a diffusion term is straightforward. For the prey, a similar term can also be added. Clearly, the reaction-diffusion scheme constitutes only an approximation of the above described settings. It could be regarded as an approximation of a cellular automata model. Implicitly, then, the grid size is assumed to be always much larger than the average size of the herd and at least of the size of the much larger territory in which it wanders. We need also to keep in mind the previous remark, that one herd can migrate into a new pasture, where perhaps another group of individuals of the same population lives, and can easily be accepted to share the food. The evidence available from biology shows that the herbivores in the African savannas drift to find new pastures, with their predators eventually following them. In Valeix et al. (2009), for instance, it is shown that all kind of herbivores seek more open habitats preferentially when predators are nearby, so that predators' behavior can structure the African herbivore communities and thus the whole savanna ecosystems. Thus this movement occurs throughout their lifetime, as feeding does, and therefore the time scales of the two phenomena in consideration, migration and predation, are of the same order. A time scale separation thus does not occur. Note also that from the same source, we gather that intermingling for the herbivores does not constitute a "social" problem, other than the standard intraspecific competition for the resources, which in our system (1–2) is modeled via the classical logistic term (Thaker et al., 2010, 2011).

Here we thus want to extend (1–2) to space. Therefore each variable will be a function of time and space location, $G(x, y, t)$ and $F(x, y, t)$. We assume again that the prey G gather together, while the predators F still go around loose. Ignoring t for the moment, let $G(U)$ then denote the size of the prey population at location $U = (x, y)$ **gathered together to form one single patch at that location**. $F(U)$ is the total loose predator population at location U. Diffusion means that some of the prey population at location U will move toward a neighboring location W incrementing the number of prey there, or better incrementing the size of the single patch present at W. **In fact in both places,**

U **and** W**, there is always only one prey patch. Also, as mentioned, the spatial location is assumed much larger than the average herd size, so that some free ground in between the herds is always present**.

With these assumptions it is meaningful to write down the following general reaction-diffusion model on the plane, in which Δ represents the Laplacian operator,

$$\frac{\partial G(X,Y,\tau)}{\partial \tau} = r\left(1-\frac{G(X,Y,\tau)}{K}\right)G(X,Y,\tau) \tag{17}$$
$$-aG(X,Y,\tau)^{\alpha}F(X,Y,\tau)+\delta_G\Delta G(X,Y,\tau)\ ,$$
$$\frac{\partial F(X,Y,\tau)}{\partial \tau} = \left(aeG(X,Y,\tau)^{\alpha}-m\right)F(X,Y,\tau)+\delta_F\Delta F(X,Y,\tau)\ . \tag{18}$$

Here δ_G and δ_F denote the diffusivities respectevely of prey and predators. Again, it differs from the classical ones due to the presence of the nonstandard predation terms in the reaction part.

We now nondimensionalize the one spatial dimensional version of system (17) via the following rescaling: $G(\tau)=KB(t)$, $F(\tau)=\omega V(t)$, $\tau=\chi t$, $X=\gamma x$. Letting then

$$\chi=\frac{1}{aeK^{\alpha}},\quad \omega=\frac{1}{aK^{\alpha-1}\chi}=eK,\quad \gamma=\sqrt{\chi\delta_G}$$

and defining the new nondimensional parameters

$$\mu=\frac{m}{aeK^{\alpha}},\quad \theta=\frac{r}{aeK^{\alpha}},\quad D=\frac{\delta_F}{\delta_G}$$

we get

$$\frac{\partial B(x,t)}{\partial t} = \theta B(x,t)\left(1-B(x,t)\right)-B(x,t)^{\alpha}V(x,t)+\frac{\partial^2 B(x,t)}{\partial x^2}\ ,$$
$$\frac{\partial V(x,t)}{\partial t} = V(x,t)\left(B(x,t)^{\alpha}-\mu\right)+D\frac{\partial^2 V(x,t)}{\partial x^2}\ . \tag{19}$$

The equilibria of the space independent version of the nondimensionalized model (19) are the points $Q_1=(0,0)$, $Q_2=(1,0)$, and $Q_3\equiv(G_a^*,F_a^*)$ with

$$G_a^*=\mu^{\frac{1}{\alpha}},\quad F_a^*=\theta\mu^{\frac{1}{\alpha}-1}\left(1-\mu^{\frac{1}{\alpha}}\right).$$

Since the nonspatial counterpart of the system (19) is effectively the original system (1–2) considered for the special choice of parameters, i.e. for $a=e=K=1$, the results of Section 2.1 immediately apply here with $\rho=\mu^{1/\alpha}$. In particular, the first two equilibria are unconditionally feasible, Q_2 is stable for $\mu>1$ and unstable otherwise. Figure 2 shows the phase portraits of the local system in the two qualitatively different cases $\mu<1$ and $\mu>1$. Q_3 is feasible for

$$\mu<1\ , \tag{20}$$

and it is stable for

$$1>\mu>\left(\frac{1-\alpha}{2-\alpha}\right)^{\alpha}\equiv\mu_H\ . \tag{21}$$

The Hopf bifurcation arises at $\mu=\mu_H$. A further decrease in μ leads to the limit cycle disappearing as a result of a nonlocal bifurcation at a certain μ_*. Based on the results of numerical simulation of the nonspatial counterpart of the nondimensionalized system (19) performed for $\theta=1$ and $\alpha=0.5$, we roughly estimate its value as $\mu_*\approx 0.55$.

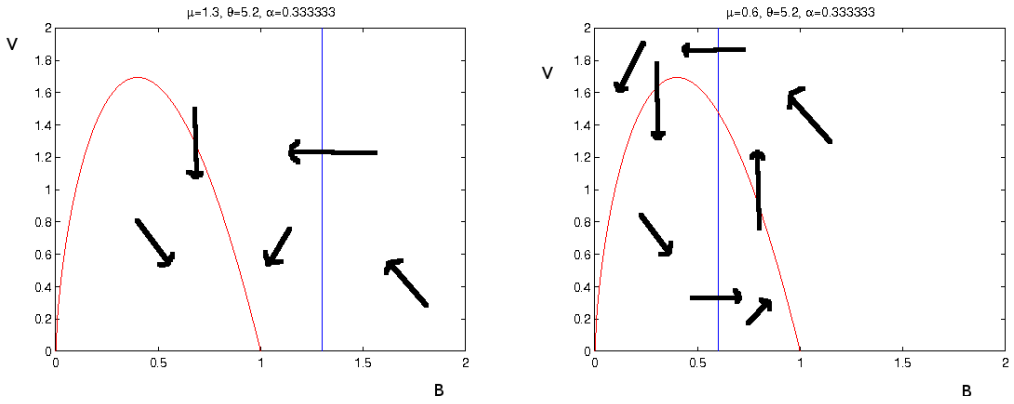

Figure 2: Phase portraits of the local nondimensional system (19) in the two cases $\mu = 1.3 > 1$ (left) and $\mu = 0.6 < 1$ (right) for $\theta = 5.2$ and $\alpha = \frac{1}{3}$.

3 Simulation results and preliminary discussion

The system (17) can unlikely be studied analytically, so we use computer simulations instead. For numerical simulations we use the forward finite difference method, with temporal stepsize chosen so as to satisfy the von Neumann stability condition,

$$\max\{1, D\}\frac{\Delta t}{\Delta x^2} < \frac{1}{2}.$$

Numerical simulations are carried out in a spatial domain $0 < x < L_x$ with $\Delta x = 1$ and time-step $\Delta t = 0.01$. The homogeneous Neumann condition is used as boundary condition over the whole perimeter of the domain. For the initial conditions, we use constant values for both populations, concentrating the prey in one half of the space domain. The predators are distributed instead in a smaller interval located at the center of the domain and partly overlapping with the prey, see Figure 3. To check the robustness of the simulation results, the numerical experiments have been repeated with smaller timesteps without any qualitative change in the final outcomes.

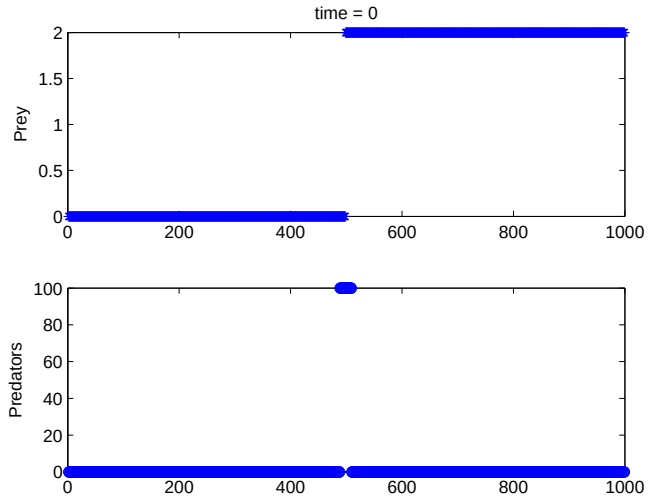

Figure 3: System's initial configuration for all the simulations.

We report here the main results of our simulations. In all cases, we kept $\alpha = 0.5$ as it allows an immediate geometrical interpretation of the grouping behavior of the prey (see Section 2.1); in this case, in the nonspatial system the Hopf bifurcation takes place at $\mu_H = \frac{1}{\sqrt{3}} \approx 0.58$. We used two values for the the diffusion coefficient, larger predators diffusivity $D = 3.5$ and the opposite case of higher prey diffusivity $D = 0.35$, and we let the remaining two parameters vary in wide ranges: for μ we used the values 2.5, 1.5, 0.8, 0.5, 0.2; for θ, we used 15.3, 5.3, 1.3, 0.4, combining then the results. The simulations were initially run for the domain size $L_x = 1000$ but in some cases the size has been extended to 3000, 6000 and even occasionally to 10000 in order to check the sensitivity of the simulations results to the domain size.

Some typical results are shown in Figs. 4–10. All the figures are designed in the same way: the snapshot of the final densities in space is shown in the left column, while the right column pictures contain the time series of the populations. The stopping times are case-dependent and therefore not uniform across the various simulations. Also the prey are always represented in the top row, the predators in the bottom one.

We obtained clear-cut situations almost in every case, with results reported in Table 1 for the selected choices of the diffusivity D. We discuss at first the case of larger relative predator diffusivity, $D = 3.5$, top part of Table 1. Here, we found that the system's final outcome hinges on the value of predators mortality μ only, independently of the prey reproductivity θ, see Table 1. For $\mu > 1$, according to what happens for the system with no space description, the predators are eradicated and the prey settle at their carrying

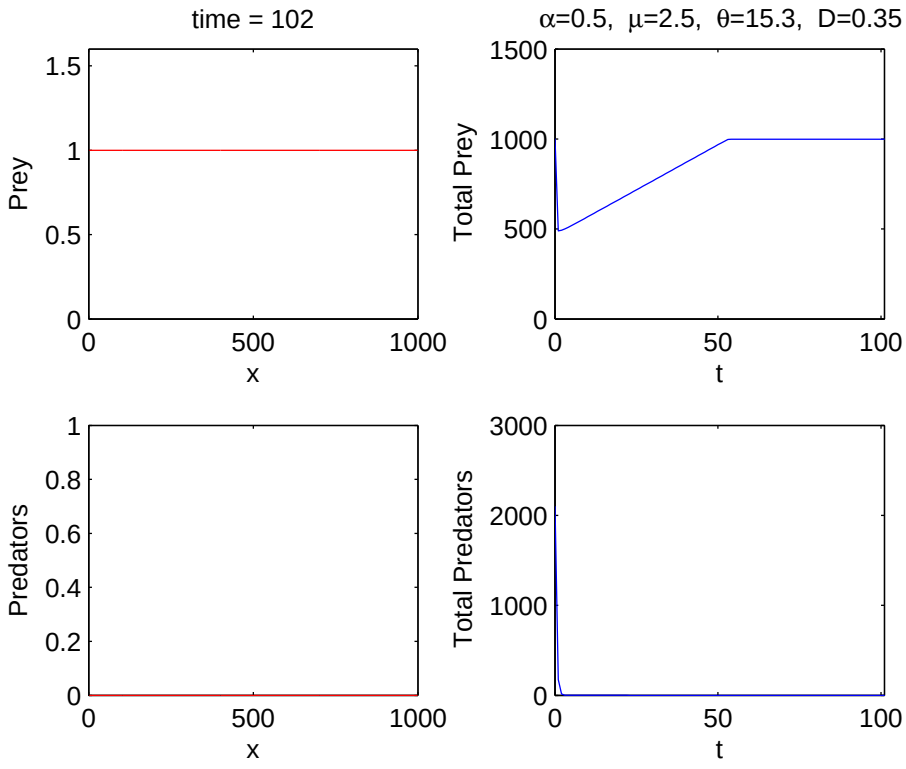

Figure 4: Settling time toward prey-only equilibrium, at carrying capacity for the parameter values: $D = 0.35$, $\mu = 2.5$, $\theta = 15.3$. On the left column, the densities as function of space, on the right column the whole populations as function of time.

capacity. This happens also when the space structure is considered. Namely this settling occurs at every location in space, Figure 4. For intermediate values $\mu_H < \mu = 0.8, 0.9 < 1$ the system locally settles at coexistence, at every space location, third and fourth rows of Table 1, and the resulting space system therefore does not show any pattern formation, as expected. For a lower value $\mu = 0.5 < \mu_* < \mu_H$, instead, persistent oscillations arise and these in space lead to patterns, Figure 5. Interestingly, for these parameter values the only attractor in the corresponding nonspatial system is the extinction state; the system's persistence is therefore essentially an effect of space. Finally, for a still lower value of the dimensionless mortality μ, the system is not capable of exhibiting persistent oscillations anymore and the same behavior is inherited by the spatial model, since it ultimately gets extinguished everywhere in the spatial domain, Fig. 6.

For the case in which prey diffuse more rapidly than predators, i.e. for $D = 0.35$ (bottom part of Table 1), the situation is similar as for the predators' dominating diffusivity, except for $\mu = 0.5$ where we have found two types of behavior depending on the value of θ, namely, formation of self-sustained patterns and extinction. Interestingly, in the latter case we have discovered that initially patterns are formed, but then the system collapses throughout the space domain, which is hardly surprising taking into account that for small values of μ the only attractor in the system is the extinction state. We have also tried one order of magnitude larger prey reproductive rate $\theta = 115.3$ for the case $D = 3.5$, to see if also in case of faster diffusing predators the model shows the same feature and found persistent patterns for long times. Instead, for the same parameter values and prey

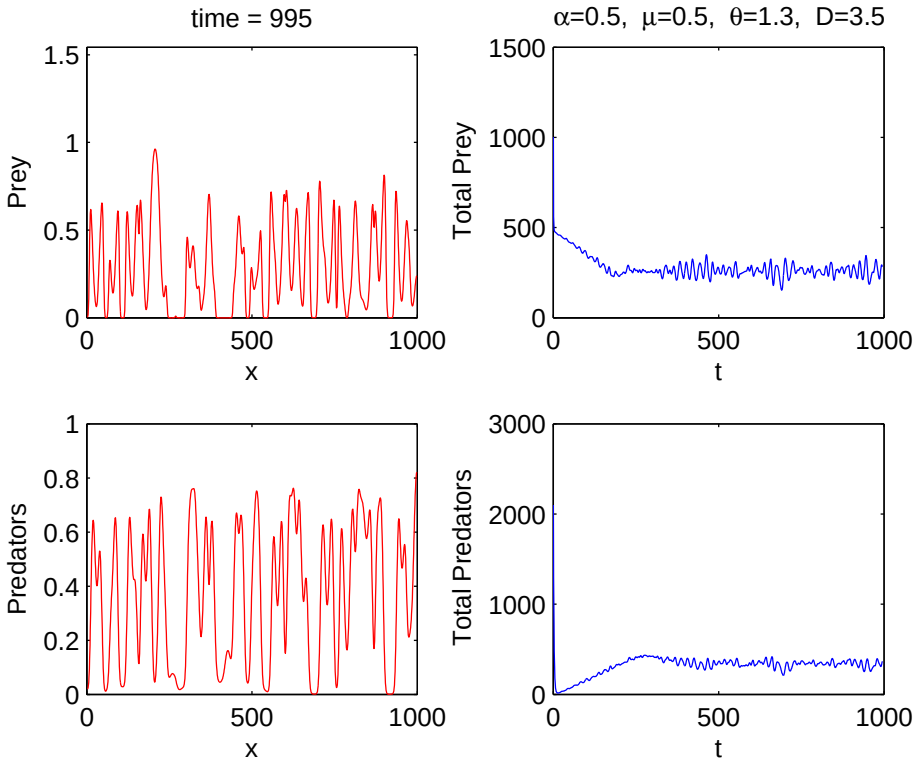

Figure 5: Persistent oscillations arise leading to patterns in space for the parameter values: $D = 3.5$, $\mu = 0.5$, $\theta = 1.3$. On the left column, the densities as function of space, on the right column the whole populations as function of time.

diffusing faster, $D = 0.35$, again the system is doomed. In Figures 7 and 8 we respectively show the patterns generated and those just before extinction. The wavefront of the trivial equilibrium in Fig. 8 moves from right to left.

We then explored the conjecture whether it is the effect of the boundaries that makes the system collapse. We have thus enlarged the simulation domain to assess for possible changes in the system's behavior. Interestingly, for $\alpha = 0.5$ and $\theta = 1.52$ in the domain $[0, 1000]$ persistent patterns develop that show the total populations having also a cyclic nature, see Figure 9, but on further scrutiny this is seen as an artifact. In fact, running the simulations in $[0, 3000]$ up to a larger time this cyclic behavior of the total populations dampens, see Fig. 10.

In Tables 2-5 we summarize the times the system takes toward attaining equilibria as a function of the predators mortality, the prey reproductivity, and the size of the space domain, for two values of the diffusivity. As a general obvious remark, we find that the larger the domain, i.e. the complexity of the computations, the longer the time for the system to attain the steady state. The settling time is estimated, for instance in Figure 4, as the point at which the plot of the total prey population has a kink, and becomes steady, given that the total predator population has already reached its (vanishing) equilibrium. The corresponding nondimensional time can be read off on the bottom axis.

In Table 2, the settling times, empirically estimated as stated above, toward the prey only equilibrium (BCC), the predator-prey coexistence at steady state (CSS) and the system's extinction (EXT) are compared. As mentioned above, the role of predators'

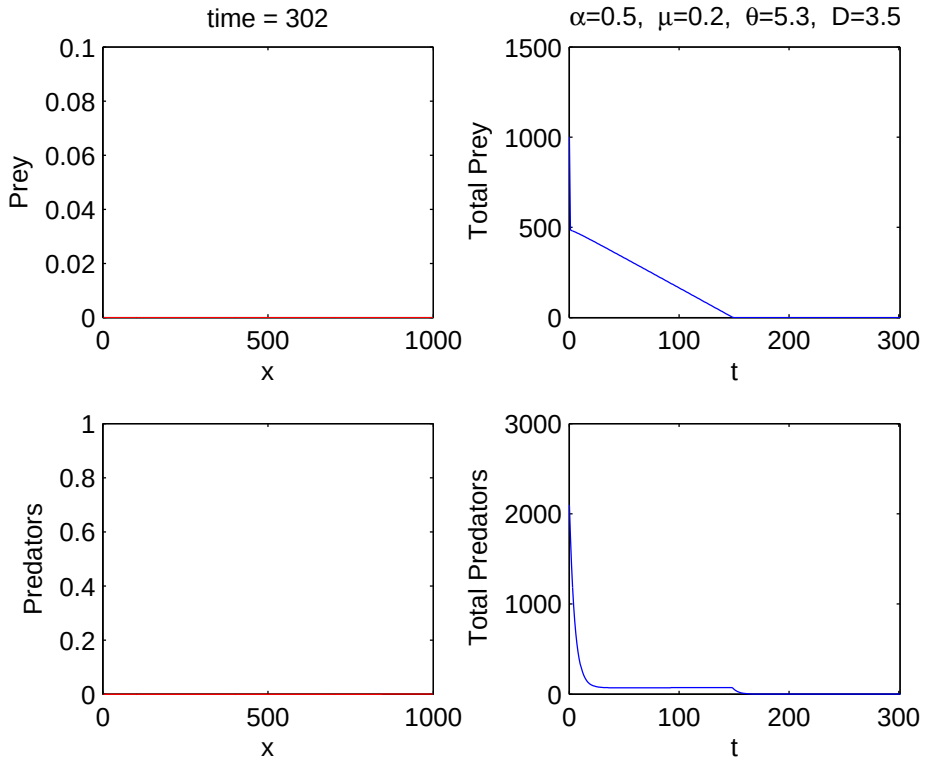

Figure 6: The system becomes extinct for the parameter values: $D = 3.5$, $\mu = 0.2$, $\theta = 5.3$. On the left column, the densities as function of space, on the right column the whole populations as function of time.

mortality is mainly to establish the type of the final simulation result. For the case BCC, the prey reproduction rate θ seems instead to influence more the outcome, as it is natural to expect. The higher it is, the faster the prey will reach the carrying capacity, in both cases when they diffuse faster (top portion of the Table) and slower (bottom part of the Table) than predators. The reaching of coexistence, rows labeled CSS, is hardly infuenced by θ, except for very low values of it, which somewhat delay the attainment of steady state. This is also evident, since the prey do not reproduce fast and therefore their total population attains more slowly the carrying capacity. It is very interesting instead the fact that for the extinction, the faster the prey reproduce, the faster the system collapses. This is probably to be ascribed to the fact that larger prey abundance allows growth of the predators, which then hunt the prey more and wipe them out, thus leading to the final system's collapse. The times toward extinction are different for the two diffusivities, here apparently slower when the prey diffuse faster. Again, an interpretation could be the fact that in this way they may be more able to escape hunting than for the situation in which predators diffuse faster. As function of the predators' mortality, μ instead, the reaching of the prey-only equilibrium (BCC) does not seem to be significantly affected, as it should be expected. A larger predators mortality instead makes the time to attain coexistence equilibrium (CSS) much longer, when the prey diffuse more rapidly. In the converse case, the same situation occurs, but the differences between the times to equilibrium are smaller. Extinction times (EXT) appear instead to be hardly affected by the predators' mortality.

In Table 3, the extinction times are compared as functions of the space domain. The

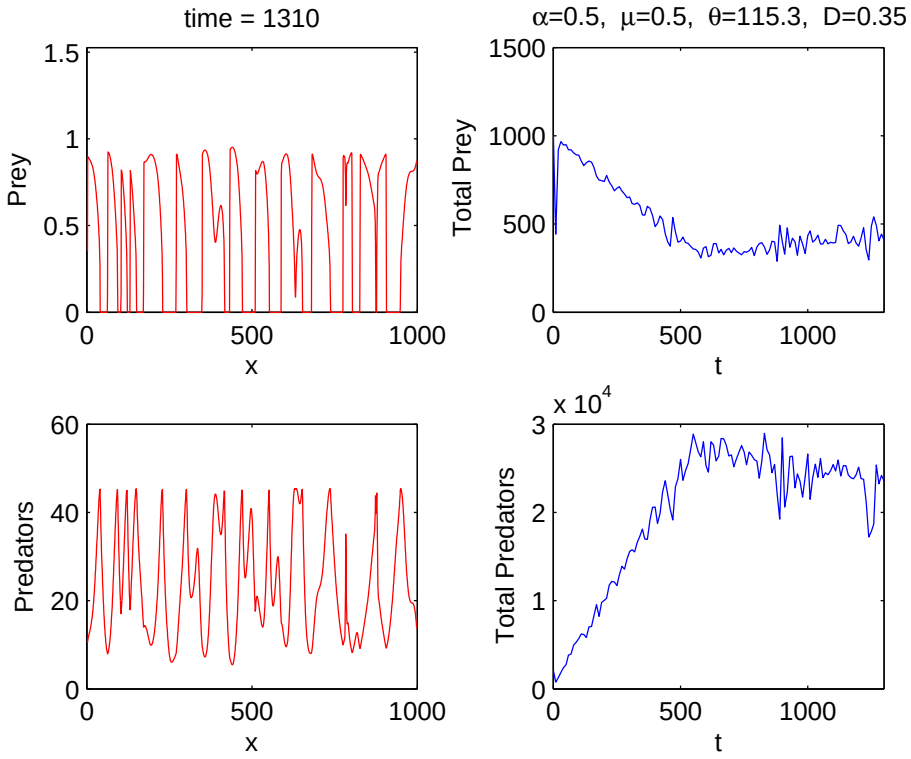

Figure 7: Patterns generated in space (right column) for the parameter values: $D = 0.35$, $\mu = 0.5$, $\theta = 115.3$ at time $t = 1310$.

predators mortality is fixed, and the prey reproduction has little or no effect on the extinction time, always making it shorter whenever it is higher, for the reason discussed above. The larger the space domain instead, the longer the system can survive, a fact that occurs also when prey diffuse faster. The net result is that the extinction time is dependent on the size of the space domain, but the ultimate system's behavior is not affected.

In Table 4, the time to reach coexistence is shown as function of the space domain. The irrelevance of the prey reproduction rate is retained also in larger domains in almost every situation. Further, the larger the domain, the longer the system takes to settle. But a higher predators diffusion favors faster settling times.

Table 5 contains the results for the prey-only equilibrium. Here a larger prey reproduction implies quicker convergence toward carrying capacity, as it should be expected. The larger the space domain however, the more time is required. Clearly, the results are essentially independent of the predators diffusivity, since the latter are wiped out.

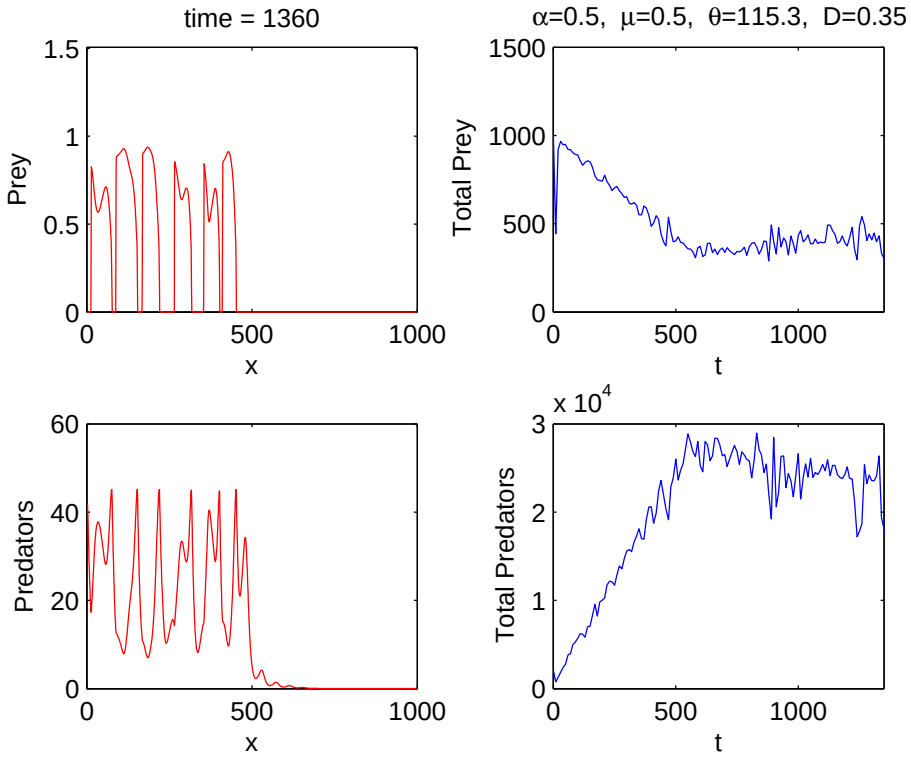

Figure 8: The spatial patterns generated in Fig. 7 become extinguished as the trivial equilibrium propagates in space from right to left (right column); parameter values: $D = 0.35$, $\mu = 0.5$, $\theta = 115.3$. The extinction starts slightly after the situation of Fig. 7 and is here pictured at time $t = 1360$. The whole ecosystem will collapse by time $t = 1500$.

	$\mu \setminus \theta$	15.3	5.3	1.3	0.4
$D = 3.5$	2.5	BCC	BCC	BCC	BCC
	1.5	BCC	BCC	BCC	BCC
	0.9	CSS	CSS	CSS	CSS
	0.8	CSS	CSS	CSS	CSS
	0.5	CPP	CPP	CPP	CPP
	0.3	EXT	EXT	EXT	EXT
	0.2	EXT	EXT	EXT	EXT
$D = 0.35$	2.5	BCC	BCC	BCC	BCC
	1.5	BCC	BCC	BCC	BCC
	0.9	CSS	CSS	CSS	CSS
	0.8	CSS	CSS	CSS	CSS
	0.5	EXTAP	EXTAP	CPP	CPP
	0.3	EXT	EXT	EXT	EXT
	0.2	EXT	EXT	EXT	EXT

Table 1: Simulation results. BCC: the prey at carrying capacity, extinction of the predators; CSS: coexistence at steady state; CPP: coexistence through persistent patterns; EXT: ecosystem extinction; EXTAP: extinction after pattern formation.

		$\mu \setminus \theta$	15.3	5.3	1.3	0.4
$D = 0.35$	BCC	2.5	60	120	230	440
	BCC	1.5	60	110	240	420
	CSS	0.9	1400	1400	1400	1400
	CSS	0.8	950	950	1000	1000
	EXT	0.3	470	470	550	850
	EXT	0.2	460	470	550	800
$D = 3.5$	BCC	2.5	60	110	240	420
	BCC	1.5	60	110	230	420
	CSS	0.9	500	500	500	520
	CSS	0.8	340	340	350	450
	EXT	0.3	260	260	260	260
	EXT	0.2	230	320	320	320

Table 2: Comparison of settling times for the cases of higher prey diffusivity and higher predators diffusivity. BCC, the prey attain carrying capacity, predators get extinguished; CSS, coexistence at steady state; EXT, system's extinction.

	domain $\setminus$ θ	15.3	5.3	1.3	0.4
$D = 0.35$	$[0, 1000]$	460	470	550	800
	$[0, 3000]$	1350	1350	1450	1650
	$[0, 6000]$	2700	2700	2750	3000
	$[0, 10000]$	4500	4450	4520	4770
$D = 3.5$	$[0, 1000]$	230	320	320	320
	$[0, 3000]$	520	520	520	520
	$[0, 6000]$	1100	900	900	900
	$[0, 10000]$	1550	1550	1550	1550

Table 3: Extinction times versus domain size for some selected values of θ and of space ranges, when $\mu = 0.2$.

	domain $\setminus$ θ	15.3	5.3	1.3	0.4
$D = 0.35$	$[0, 1000]$	950	950	1000	1000
	$[0, 3000]$	2800	2800	2800	2300
	$[0, 6000]$	5600	5600	5600	5600
	$[0, 10000]$	9300	9300	9300	9300
$D = 3.5$	$[0, 1000]$	340	340	350	450
	$[0, 3000]$	950	950	950	1250
	$[0, 6000]$	1840	1840	1840	2450
	$[0, 10000]$	3050	3050	3050	4000

Table 4: Settling times to coexistence at steady state versus domain size for some selected values of θ and of space ranges, when $\mu = 0.8$.

	domain $\setminus$ θ	15.3	5.3	1.3	0.4
$D = 0.35$	$[0, 1000]$	60	120	230	440
	$[0, 3000]$	180	310	650	1200
	$[0, 6000]$	350	600	1250	2370
	$[0, 10000]$	560	1000	2150	3950
$D = 3.5$	$[0, 1000]$	60	110	230	440
	$[0, 3000]$	180	310	650	1200
	$[0, 6000]$	350	600	1250	2370
	$[0, 10000]$	560	1000	2150	3950

Table 5: Settling times to prey only equilibrium versus domain size for some selected values of θ and of space ranges, when $\mu = 2.5$.

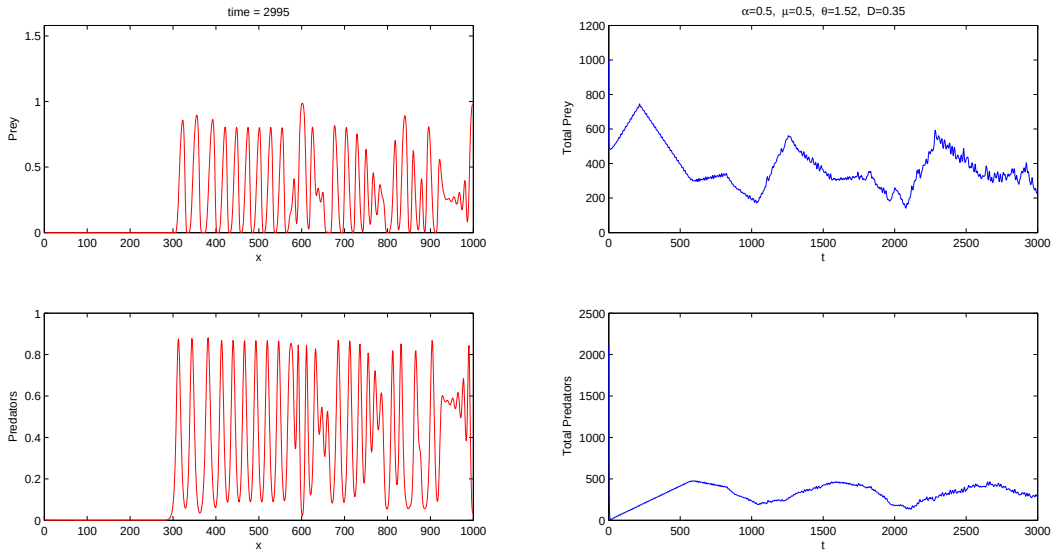

Figure 9: Persistent spatial patterns (left) develop and the total populations (right) seem to behave cyclically for the parameter values: $D = 0.35$, $\mu = 0.5$, $\theta = 1.52$. On the left column, the densities as function of space, on the right column the whole populations as function of time.

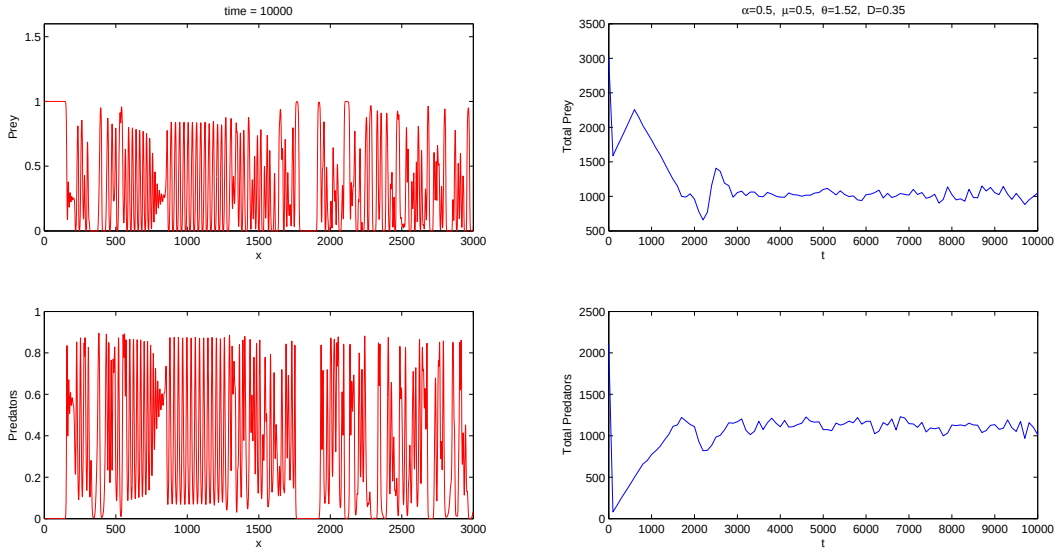

Figure 10: In reference to Fig. 9, over a larger space domain and over a longer simulation run up to time $t = 10000$, the cycles of the total populations in Fig. 9 are lost, showing that it is mainly an effect of the boundaries. In fact the earlier kinks in the previous Fig. 9 correspond to the times at which the population wave hits the boundaries. This picture holds for the very same parameter values: $D = 0.35$, $\mu = 0.5$, $\theta = 1.52$. On the left column, the densities as function of space, on the right column the whole populations as function of time.

θ	15.3	5.3	1.3	0.4
time	0.4	1.2	5	18

Table 6: Settling times for the prey to carrying capacity in the nondimensional model for some selected values of θ, for the same initial conditions chosen for the spatial model, but in absence of predators.

4 Concluding Remarks

The dynamics of social interactions in animal population and communities and their impact on fitness and population persistence, both within one generation and on a multi-generation scale, have recently been attracting an increasing attention. In theoretical and modeling studies, they are usually investigated using an individual based approach, i.e. by following the behaviour, movement and fate of each individual explicitly, (Maynard Smith and Price, 1973; Clark, 1993). This approach has proved to be very useful to identify the main tendencies in the dynamics of the corresponding communities. However, this approach is essentially simulation-based. It is therefore very difficult to obtain general system's properties in a wider parameter range.

In order to overcome these inherent drawbacks of the individual based approach, the impact of social interactions can alternatively be studied in terms of the corresponding population densities, (Fryxell and Lundberg, 1997; Petrovskii and Blackshaw, 2003). In this paper, we use this approach to consider the consequences of animal grouping as a response to predation. We describe the system by a prey-predator type model where predation has an unconventional functional form. We first consider the properties of the nonspatial system and show that it exhibits a peculiar behaviour not observed in the traditional Rosenzweig-McArthur type prey-predator models. In particular, in a certain parameter range the phase plane of the system appears to be split into two parts. While for most of the plane the extinction state $(0, 0)$ acts as a saddle point, there exists a curvilinear sector adjoining the vertical axis for which the extinction state acts as an attractor. Note that similar properties have earlier been observed in ratio-dependent systems (Jost et al., 1999) but never in prey-dependent ones.

We then explore the properties of the spatially explicit system by means of extensive computer simulations. For the spatiotemporal dynamics, our main findings can be summarized as follows:

- Settling of species toward trivial equilibria could often be preceded by transient behaviors, which may be very long, depending on the system parameters and the size of the space domain. The system may be thriving on the scale of $t \sim 10^3$ to 10^4, see fourth and last rows of Tables 3-5, exhibiting a significant growth in the population sizes before it finally collapses.

Note that it is not straightforward to compare the timings of the local model with the space-dependent ones, because all the simulations and the corresponding results in the Tables have been obtained using nonhomogeneous initial conditions in space. Therefore the corresponding situation cannot be mimicked at the local level: either initially the predators are zero or at a nonzero level, and the behavior of the local model will correspondingly either tend to the predator-free equilibrium, or possibly to coexistence, or

even become extinct. What the Tables contain are the settling times of the whole populations in the spatial domain. Thus, only relative comparisons are possible. However, the initial conditions are chosen so that over 1% of the domain prey and predators coexist, over another 1% of the domain only predators are present, over 49% of the domain only prey are present, all these populations being always at constant level, and the remaining 49% of the spatial domain is empty, Figure 3. In view of the fact that the overwhelming nontrivial initial spatial condition contains only prey, in Table 6 we provide the settling times of the prey to their carrying capacity for the nondimensional model, starting from the very same initial condition of the spatial model, when predators are absent. The table is a function only of the nondimensionalized prey reproductive rate θ, as evidently in this case the nondimensionalized predators' mortality μ plays no role. By comparing the results of Tables 2-5 with those in Table 6, the claim of much longer settling times in the spatial model is thus evident. Turning now to relative comparisons, from Tables 2 and 4 we find that the prey settle to the predator-free equilibrium much faster than the sytem takes to get extinguished, if the prey diffuses faster than the predators. If the reproductive rate is high enough, $\theta = 15.3$ for instance, the predator-free equilibrium is attained in about a eighth of the time for system's extinction. For low values of the reproductive rate, $\theta = 0.4$, the ratio becomes about one half. Reaching the coexistence state however, Table 4, in such situation requires 16 times the settling time to the predator-free equilibrium for a fast reproducing prey population, and about 2.5 times in case of the prey low reproductive rate. The general picture holds also in case the predators diffuse faster, although in such case coexistence can be attained in about a third of the time of the previous case, thereby reducing by the same ratio the comparisons. Here the time to reach the prey-only equilibrium is not affected by the predators' diffusivity higher than the prey's, as it can easily be foreseen, since the predators vanish. In Tables 4-5 observe that the settling time to the different equilibria grows about linearly with the size of the domain. When the settling times toward coexistence are considered, a marked decrease occurs for the largest domain in case predators diffuse faster. Once more note that for the settling times toward the prey-only equilibrium point clearly the predators' have no role, the entries in the top and bottom parts of Table 5 coincide. The times exhibit instead a marked decrease for increasing prey reproduction rates starting from their lowest value $\theta = 0.4$.

- Persistent irregular oscillations are discovered as temporal patterns among the cumulative populations evolving in time. This feature should be expected, as it is well-known that limit cycles in the local model induce patterns in its spatial counterpart; see Malchow et al. (2008). Let us note, however, that a comprehensive theory relating the existence of local oscillations to pattern formation in space is largely lacking and hence the system (19) provides a valuable extension of the existing results.

- The spatial system disappearance provides a sufficient condition for its non-spatial counterpart: whenever the conditions for system collapse at the local level are satisfied also its spatial counterpart gets extinguished. Extinction of the system can also be enhanced by predators diffusing faster than the prey, as it takes about half the time of the opposite case. In Table 3 the extinction time grows about linearly with the size of the domain, but if the prey diffuse faster there is a sharp reduction when the reproduction rate grows from the lowest value $\theta = 0.4$ and thereafter becomes

almost constant. This is more marked for low-sized domains. For the predators diffusing faster instead, the timings are essentially constant.

With regard to species extinction observed in numerical simulations, we ascribe it to the impact of two factors. Firstly, extinction of species is obviously predicted by Theorem 1 when the densities fall into the corresponding domain of the phase plane, i.e. into the basin of the extinction state. Secondly, in a broad parameter range, the population oscillations show a large amplitude so that the limit cycle lies close to the phase plane boundaries. The observed extinction of species than can happen as a result of these large oscillations which may bring the population densities to values very close to zero for the prey and very large for the predators. When this happens, the trajectories will fall into the basin of attraction of the origin. Note that this behavior is fully relevant to what actually happens in ecosystems due to the impact of stochastic factors, even though those environmental factors are not included explicitly into our model.

Thus the spatial system is **less** likely to become extinct than the local one. Persistence in the spatial domain is obtained via pattern formation, although in some cases, when the prey diffuse faster, these lead to system's extinction anyway. The prey survive either alone or at coexistence state or via the patterns. In the former case the predator-free equilibrium is reached under the very same theoretical conditions that imply it in the local model.

The equilibria of the system are obtained in general through features such as waves of prey propagating with predators on their pursuit. Thus the proposed system exhibits excitability properties, in which pulses propagate along the spatial one-dimensional direction. Models of related nature and similar conclusions have recently been investigated in the literature, see for instance Petrovskii et al. (2005); Morozov and Petrovskii (2009); Banerjee and Petrovskii (2011). Also ecoepidemic models involving prey group defense have been proposed and examined, and show also interesting phenomena as the triggering of persistent oscillations, (Venturino, 2011). Extensions of the present model could consider competing interactions or those of mutualistic nature.

Acknowledgments: EV thankfully acknowledges very useful discussions with Horst Malchow (Osnabrück), Frank Hilker (Bath) and his biologist colleague Guido Badino (Torino). SP is thankful to Andrew Morozov (Leicester) for useful comments and to Ivan Tyukin (Leicester) for a discussion of mixed stability.

References

Ajraldi, V., M. Pittavino, and E. Venturino (2011). Modelling herd behavior in population systems. *Nonlinear Analysis Real World Applications 12*, 2319–2338.

Ajraldi, V. and E. Venturino (2009). Mimicking spatial effects in predator-prey models with group defense. In V.-A. J., A. P., O. S., V. E., and W. B. (Eds.), *Proceedings of the 2009 International Conference on Computational and Mathematical Methods in Science and Engineering*, pp. 57–66. Salamanca: CMMSE.

Allee, W. (1938). *The Social Life of Animals*. New York: Norton and Co.

Axelrod, R. (1997). *The Complexity of Cooperation: Agent-Based Models of Competition and Collaboration*. Princeton: Princeton University Press.

Banerjee, M. and S. Petrovskii (2011). Self-organised spatial patterns and chaos in a ratio-dependent predator-prey system. *Theor. Ecol. 4*, 37–53.

Bertram, B. (1978). Living in groups. predators and prey. In J. Krebs and N. Davies (Eds.), *Behavioural Ecology*, pp. 64–96. Oxford: Blackwell.

Bode, N. W. F., J. J. Faria, D. W. Franks, J. Krause, and A. J. Wood (2010). How perceived threat increases synchronization in collectively moving animal groups. *Proc. R. Soc. B 227*, 3065–3070.

Bode, N. W. F., A. J. Wood, and D. W. Franks (2011). Social networks and models for collective motion in animals. *Behavioral Ecology and Sociobiology 65*, 117–130.

Caro, T. (2005). *Antipredator Defenses in Birds and Mammals*. Chicago: University of Chicago Press.

Clark, C. W. (1993). Dynamic models of behavior: an extension of life history theory. *Trends Ecol. Evol. 8*, 205–209.

Elgar, M. (1989). Predator vigilance and group size in mammals and birds: a critical review of the empirical evidence. *Biol Rev. Camb. Philos Soc. 64*, 13–33.

Fernö, A., T. Pitcher, W. Melle, L. Nøttestad, S. Mackinson, C. Hollingworth, and O. Misund (1998). The challenge of the herring in the norwegian sea: making optimal collective spatial decisions. *SARSIA 83*, 149–167.

FitzGibbon, C. (1989). A cost to individuals with reduced vigilance in groups of thomson's gazelles hunted by cheetahs. *Animal Behaviour 37(3)*, 508–510.

FitzGibbon, C. (1990). Mixed-species grouping in thomson's and grant's gazelles: the antipredator benefits. *Animal Behaviour 39(6)*, 1116–1126.

Freeman, L., S. Freeman, and A. Romney (1992). The implications of social structure for dominance hierarchies in red deer, it Cervus elaphus l. *Anim. Behav. 44*, 239–245.

Fryxell, J. and P. Lundberg (1997). *Individual Behaviour and Community Dynamics*. London: Chapman & Hall.

Fryxell, J., A. Mosser, A. Sinclair, and C. Packer (2007). Group formation stabilizes predator-prey dynamics. *Nature 449(7165)*, 1041–1043.

Grünbaum, D. and A. Okubo (1994). Modelling social animal aggregations. In S. A. Levin (Ed.), *Frontiers in mathematical biology*, pp. 296–325. Berlin: Springer.

Halil, H. (2002). *Nonlinear Systems (3rd edition)*. New Jersey: Prentice Hall.

Jost, C., O. Arino, and R. Arditi (1999). About deterministic extinction in ratio-dependent predator-prey model. *Bull Math Biol 61*, 19–32.

Macal, C. M. and M. J. North (2009). Tutorial on agent-based modeling and simulation part 2: how to model with agents. In L. F. Perrone, F. P. Wieland, J. Liu, B. G. Lawson, D. M. Nicol, and R. M. Fujimoto (Eds.), *Proceedings of the 2006 Winter Simulation Conference*, pp. 73–83. IEEE.

Magurran, A. (1990). The adaptive significance of schooling as an anti-predator defence in fish. *Ann.Zool. Fennici 27*, 51–66.

Malchow, H., S. Petrovsky, and E. Venturino (2008). *Spatiotemporal patterns in Ecology and Epidemiology*. Boca Raton: CRC.

Maynard Smith, J. and G. Price (1973). The logic of animal conflict. *Nature 246*, 15–18.

Morozov, A. and S. Petrovskii (2009). Excitable population dynamics, biological control failure, and spatiotemporal pattern formation in a model ecosystem. *Bulletin of Mathematical Biology 71*, 863–887.

Petrovskii, S. and R. Blackshaw (2003). Behaviourally structured populations persist longer under harsh environmental conditions. *Ecol. Lett. 6*, 455–462.

Petrovskii, S., A. Morozov, and B.-L. Li (2005). Regimes of biological invasion in a predator-prey system with the allee effect. *Bulletin of Mathematical Biology 67*, 637–661.

Sapolsky, R. (2005). The influence of social hierarchy on primate health. *Science 308*, 648–652.

Sendova-Franks, A., N. Franks, and N. Britton (2002). The role of competition in task switching during colony emigration in the ant *leptothorax albipennis*. *Anim. Behav. 63*, 715–725.

Thaker, M., A. Vanak, C. Owen, M. Ogden, S. Niemann, and R. Slotow (2011). Minimizing predation risk in a landscape of multiple predators: effects on the spatial distribution of african ungulates. *Ecology 92(2)*, 398–407.

Thaker, M., A. Vanak, C. Owen, and R. Slotow (2010). Group dynamics of zebra and wildebeest in a woodland savanna: effects of predation risk and habitat density. *PLoS One 5(9)*, e12758.

Valeix, M., A. Loveridge, S. Chamaillé-Jammes, Z. Davidson, F. Murindagomo, H. Fritz, and D. Macdonald (2009). Behavioral adjustments of african herbivores to predation risk by lions: spatiotemporal variations influence habitat use. *Ecology 90(1)*, 23–30.

Venturino, E. (2011). A minimal model for ecoepidemics with group defense. *J. of Biological Systems 19(4)*, 763–785.

Wilson, E. (1971). *The Insect Societies*. Cambridge: Belknap Press.

Wood, A. J. and G. J. Ackland (2007). Evolving the selfish herd: emergence of distinct aggregating strategies in an individual-based model. *Proc. R. Soc. B 274*, 1637–1642.